General Psychiatry

MicroRNA-451a is a candidate biomarker and therapeutic target for major depressive disorder

Panpan Hu,[1] Qiuchen Cao,[1] Hu Feng,[1] Yun Liu,[2] Yan Chen,[1] Jingfan Xu,[1] Weixi Feng,[1] Huaiqing Sun,[2] Huachen Ding,[3,4] Chun Wang,[3,4] Junying Gao,[1] Ming Xiao ![ORCID] [1,4]

[1]Jiangsu Key Laboratory of Neurodegeneration, Nanjing Medical University, Nanjing, Jiangsu, China
[2]Department of Neurology, The First Affiliated Hospital of Nanjing Medical University, Nanjing, Jiangsu, China
[3]Nanjing Brain Hospital Affiliated to Nanjing Medical University, Nanjing, Jiangsu, China
[4]Functional Brain Imaging Institute of Nanjing Medical University, Nanjing, Jiangsu, China

Correspondence to
Dr Ming Xiao;
mingx@njmu.edu.cn

Junying Gao;
gaojunying@njmu.edu.cn

ABSTRACT

Background Increasing evidence supports the role of microRNAs (miRNAs) in major depressive disorder (MDD), but the pathophysiological mechanism remains elusive.
Aims To explore the mechanism of microRNA-451a (miR-451a) in the pathology and behaviours of depression.
Methods Abnormal miRNAs such as miR-451a reported previously in the serum of patients with MDD were screened and then confirmed in a mouse model of depression induced by chronic restraint stress (CRS). Eight-week-old male C57BL/6 mice had miR-451a overexpression in the medial prefrontal cortex (mPFC) via adeno-associated virus serotype 9 vectors encoding a pri-mmu-miR-451a-GFP fusion protein followed by behavioural and pathological analyses. Finally, molecular biological experiments were conducted to investigate the potential mechanism of miR-451a against depression.
Results The serum levels of miRNA-451a were significantly lower in patients with MDD, with a negative correlation with the Hamilton Depression Scale scores. Additionally, a negative association between serum miR-451a and behavioural despair or anhedonia was observed in CRS mice. Notably, miR-451a expression was significantly downregulated in the mPFC of CRS-susceptible mice. Overexpressing miR-451a in the mPFC reversed the loss of dendritic spines and the depression-like phenotype of CRS mice. Mechanistically, miR-451a could inhibit CRS-induced corticotropin-releasing factor receptor 1 expression via targeting transcription factor 2, subsequently protecting dendritic spine plasticity.
Conclusions Together, these results highlighted miR-451a as a candidate biomarker and therapeutic target for MDD.

WHAT IS ALREADY KNOWN ON THIS TOPIC

⇒ Major depressive disorder (MDD), a common mental disorder, is caused by a combination of biological, genetic and psychosocial factors.
⇒ MicroRNA-451a (miR-451a) is involved in MDD, but the mechanism remains unclear.

WHAT THIS STUDY ADDS

⇒ This study found a negative correlation between serum miR-451a and behavioural despair or anhedonia in a mouse model of depression induced by chronic restraint stress (CRS).
⇒ Notably, miR-451a expression was significantly downregulated in the medial prefrontal cortex of CRS-susceptible mice.
⇒ Overexpressing miR-451a in this region reversed the loss of dendritic spines and the depression-like phenotype of CRS mice.
⇒ Mechanistically, miR-451a could inhibit CRS-induced corticotropin-releasing factor receptor 1 expression via targeting transcription factor 2, subsequently protecting dendritic spine plasticity.

HOW THIS STUDY MIGHT AFFECT RESEARCH, PRACTICE OR POLICY

⇒ This study highlights miR-451a as a candidate biomarker and therapeutic target for MDD.

INTRODUCTION

Major depressive disorder (MDD) is a common mental disorder caused by a combination of biological, genetic and psychosocial factors.[1] The key symptoms of MDD consist of depression, pessimism and negativity, loss of interest and energy, and a lack of pleasure and motivation.[2] Investigating the epigenetic factors associated with the symptoms of depression could lead to novel diagnostic and treatment options. The chronic restraint stress (CRS) model, widely used in depression research, induces depressive-like symptoms in animals through prolonged physical restraint, thereby aiding in studying neurobiological mechanisms and potential antidepressant drugs.[3]

As the main regulator of gene expression, small non-coding RNAs have attracted extensive attention for their regulatory roles in the pathogenesis of various diseases, including MDD.[4] Among them, microRNAs (miRNAs) are the most intensively investigated. MicroRNA-451a (miR-451a) is a small RNA molecule that plays a role in the post-transcriptional regulation of gene expression. It has been implicated in various neurological

disorders, including MDD and autism spectrum disorders.[5 6] Decreased miR-451a was found in plasma samples as well as in the cerebrospinal fluid (CSF) of patients with a first episode of MDD and partially recovered after ketamine treatment.[5] Conversely, another publication from Camkurt *et al*[6] reported that miR-451a was significantly upregulated in venous blood samples of depressed patients. Despite this discrepancy, both authors agreed that miR-451a could serve as a biomarker for depression. However, the exact role of miR-451a in the pathogenesis of MDD remains elusive.

In this study, we screened miRNAs associated with MDD from the literature and then validated them in serum samples from patients with MDD. We confirmed that the serum miR-451a levels in patients with MDD were significantly decreased and negatively correlated with the Hamilton Depression Scale (HAMD) score. We also compared the miR-451a levels in the serum and the medial prefrontal cortex (mPFC) between CRS mice and intact controls. We further determined whether overexpression of miR-451a in the mPFC could mitigate CRS-induced, depression-like behaviours in mice. Finally, we explored the intrinsic mechanism of miR-451a against depression.

MATERIALS AND METHODS
Patients and healthy controls

Our research included 17 healthy controls and 35 patients with a first episode of MDD (figure 1). Enrolment was open to adult men and women aged 18–65 years old. Eligible subjects required a Diagnostic and Statistical Manual of Mental Disorders Structured Clinical Interview (Fourth Edition) diagnosis of MDD[7]; screening was conducted by psychiatrists from Nanjing Brain Hospital of Nanjing Medical University. The study started in June 2018 and concluded in December 2021. HAMD (24-item version) was used to evaluate the severity of depressive symptoms, such as depression, loss of interest, decreased energy, fatigue and pain[8]; and the Hamilton Rating Scale for Anxiety (HAMA; 17-item version) was used to evaluate the severity of anxiety symptoms.[9] Patients with MDD were identified based on a score of 20 or higher on the HAMD, with the assessment conducted by an independent, trained rater. The exclusion criteria were as follows: any antidepressant treatment for more than a week, history of brain trauma, severe personality disorder, risk of suicide, pregnancy, current psychotherapy of any kind and diagnosis of bipolar disorder (figure 1). Information on enrolment is provided in online supplemental table S1,S2. The blood sample (5 mL) of patients with MDD was collected at the same time (07:00–08:00; the second day after completing the HAMD and HAMA scores) in the inpatient ward with BD Vacutainer tubes and centrifuged at 3000 *g* for 10 min at 4°C within 2 hours. The blood sample of the healthy control participants, who had no history of mental, neurological or serious physical diseases, and who volunteered to take part in this research was collected at the same time (07:00–08:00) in the Nanjing Brain Hospital of Nanjing Medical University. All participants' evaluation and blood sample collection were completed within 2 months. The serum was then aliquoted from the supernatant and stored at –80°C before further processing.

Animals

Eight-week-old male C57BL/6 mice (Animal Core Facility of Nanjing Medical University) were used for establishing the CRS model. Mice were maintained at a constant room temperature (18°C–22°C), with a controlled illumination (12:12 hours light/dark cycle), relative humidity of 30%–50%, and with food and water available ad libitum.

Establishment of the CRS mouse model

The CRS was established by restraining the mice for 5 hours per day (09:00–14:00) for 4 consecutive weeks, as previously described.[10] During CRS, the mice were kept in isolation and placed horizontally in plastic centrifuge tubes (50 mL; 3 cm in diameter and 11.5 cm in height) with 10 pinholes with a diameter of 0.5 cm on the surface of each tube for ventilation. Toilet paper was placed at the cap site to absorb mouse faeces to minimise discomfort. After the constriction was released, the mice were put back in their home cages and given ad libitum access to food and water. The control mice were left undisturbed in their home cages. The mice were protected from any physical wounding during the modelling period.
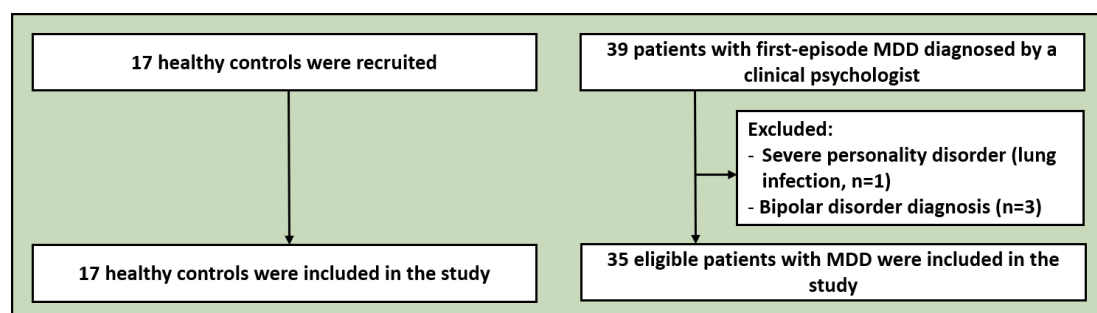
Figure 1 Flowchart of the enrolment and follow-up of subjects of the study. 17 healthy controls and 35 patients with first episode of MDD were enrolled according to the inclusion and exclusion criteria. Patients with MDD were identified based on a HAMD score of 20 or higher. HAMD, Hamilton Depression Scale; MDD, major depressive disorder.

Behavioural testing

After the modelling was completed, the mice received behavioural tests to analyse the levels of depression and anxiety in the Small Animal Behaviour Testing Laboratory of Animal Core Facility of Nanjing Medical University. Behavioural data were collected by two individuals who were unaware of animal group allocations, minimising potential experimenter-induced bias. The behavioural tests were conducted in the following order: sucrose preference test (SPT), open field test (OFT), social interaction test, elevated plus maze (EPM) test, forced swimming test (FST) and tail suspension test (online supplemental materials), for these behavioural tests gradually increased the stress in mice. Each behavioural test was conducted each day in the above order to minimise stress stimuli and potential impacts on test results. All tests were performed by experimenters who were blind to the treatment schedule.

CRS grouping

The CRS mice with a lower sugar preference rate and longer swimming immobility time than the average of the control group were categorised as belonging to the CRS susceptibility group, and those with a higher sugar preference rate and shorter swimming immobility time than the average level of the control group were termed CRS-resistant mice. Afterwards, five mice in each group were randomly selected to collect fresh brain tissue for western blot and enzyme-linked immunosorbent assay (ELISA). An additional five brain samples per group underwent Golgi silver staining to detect morphological changes in the cortical neurons. The mice that did not meet the above classification criteria were excluded from the biochemical and pathological analyses.

Viral construction and stereotaxic surgery

For overexpression of miR-451a *in vivo*, viral constructs were designed using adeno-associated virus serotype 9 (AAV9) vectors (Genechem, China), encoding a pri-mmu-miR-451a-GFP fusion protein (Ad_OE-miR-451a) or green fluorescent protein (GFP) only as a negative control, under the control of the cytomegalovirus (CMV) promoter (Ad_OE-scramble).

The mice were deeply anaesthetised with sodium pentobarbital (50 mg/kg, intraperitoneal injection) and then placed in a stereotaxic apparatus. Bilateral micro-infusions were made using a 1 µL Hamilton microsyringe with a stainless-steel infusion needle (33-gauge) into the mouse mPFC at the following coordinates: anterior-posterior: +1.90 mm; medial-lateral: ±0.5 mm; and dorsal-ventral: −2.3 mm relative to the bregma. For miR-451a overexpression experiments, a total volume of 0.25 µL of AAV-miR-451a-OE (2.0 E+13 genome copies per millilitre) or control virus was injected into the mPFC of each hemisphere over an 8 min period. The infusion needles were left inside the mPFC area during a 5 min pause to limit virus reflux. The mice recovered for 14 days before initiating the CRS procedure.

Sample and serum preparation

On the next morning after the final behavioural tests, the mice were anaesthetised and their blood was collected via the ophthalmic artery. Blood samples were allowed to coagulate in centrifuge tubes at room temperature for 30 min and subsequently centrifuged at 1500 g for 10 min. The serum was separated and stored at −80°C until the biochemical estimations were carried out. The mice were perfused transcardially with 50 mL of 0.9% saline right after blood collection, and the mPFC was quickly extracted from the whole brain, frozen by liquid nitrogen, then stored at −80°C until use.

RNA extraction and analysis

miRNA and mRNA levels were determined using real-time quantitative polymerase chain reaction (qPCR). Total RNA was isolated from human serum or from the mPFC and serum of mice using RNAiso Plus (Takara) according to the manufacturer's protocol, with minor modifications, and quantified by NanoDrop 2000 (Thermofisher, USA). Human serum miRNA detection was carried out in 384-well plates using the Q7 real-time PCR detection system (Thermofisher), and the small nucleolar RNA RNU6B was used as endogenous control. The expression of miRNAs was relativised to (ie, normalised to) the healthy control group and presented as fold change. For mouse serum miRNA analysis, the *Caenorhabditis elegans*-specific miRNA, cel-miR-39, was added to mouse serum as exogenous control. miRNAs were reverse-transcribed using a poly (A) tailing reaction and a universal cDNA synthesis kit (Sangon Biotech, China), and then qPCR was conducted using the SYBR Green MicroRNA qPCR Kit (B532461; Sangon Biotech), with the primers listed in online supplemental table S3.

Reverse transcription PCR for mRNA was carried out using a Takara PrimeScript RT Reagent Kit (no: RR036A), and mRNA expression was evaluated using a QuantiTect SYBR Green PCR Kit (RR820A; Takara, Japan) with an ABI 7300 Fast Real-Time PCR System (Applied Biosystems, Foster City, California) by real-time PCR. The results were analysed and presented relative to threshold cycle values normalised to the expression of glyceraldehyde-3-phosphate dehydrogenase (GAPDH), then converted to fold changes. The sequences of primers for real-time PCR analysis are listed in online supplemental table S4.

Western blot

Western blot analysis was performed following standard protocols. Briefly, homogenised protein of the mPFC was extracted from samples using RIPA lysis buffer (Beyotime, China) with phosphatase inhibitors (Roche, Switzerland), and concentration was determined by the Bradford assay (Beyotime). The analysis of protein was performed according to standard Sodium Dodecy Sulfate Polyacrylamide Gel Electrophoresis (SDS-PAGE). Protein was separated by 8%–15% SDS-PAGE and electrophoretically transferred onto polyvinylidene fluoride (PVDF) membranes (Millipore, USA). After blocking

for 1 hour in 5% skimmed milk in tris-buffered saline with Tween 20 (TBST), the transferred membranes were incubated with primary anti-mouse antibodies (online supplemental table S5) at 4°C overnight, and then with horseradish peroxidase (HRP)-conjugated secondary antibody for 1 hour at room temperature. The blots were visualised by an enhanced chemiluminescence (ECL) kit (Tanon, China). Values for protein levels were calculated using ImageJ (National Institutes of Health, USA) and normalised to GAPDH. Fold changes against values in the control group were calculated and used to perform statistical analysis. At least three mice in each group were used for western blot analysis.

Enzyme-linked immunosorbent assay

Quantitative determination of serum corticosterone (CORT) was performed using a commercially available ELISA kit (R&D Systems, USA) with high sensitivity (0.047 ng/mL) according to the manufacturer's instructions.

Golgi staining and dendritic spine analysis

Golgi staining was performed using the FD Rapid GolgiStain Kit (FD Neuro Technologies, USA). The dendritic spines of the neurons in layers 3–5 of mPFC were imaged using a 100× oil objective on a digital camera (Leica Microsystems, Germany). The dendritic spines on secondary or tertiary dendritic branches were analysed, and each branch was at least 10 μm in length. Five mPFC neurons per section and three sections per mouse were analysed.

FISH and immunofluorescence

For immunofluorescence, the brain sections at 15 μm containing the mPFC were blocked at room temperature for 1 hour in 5% bovine serum albumin with 0.3% phosphate-buffered saline with Tween 20 (PBST), incubated with rabbit anti-corticotropin-releasing factor receptor 1 (CRFR1) (1:600; SAB, 40785) at 4°C overnight. After phosphate buffered saline (PBS) washing, sections were incubated for 2 hours at room temperature with Alexa Fluor 555 goat anti-rabbit IgG (H+L) highly cross-adsorbed secondary antibody (1:1000; Invitrogen, 31572), then incubated for 5 min at room temperature in 1.5 μM DAPI (4′,6-diamidino-2-phenylindole; Invitrogen, D1306) and sealed with buffered PBS/glycerol.

Locked-nucleotide modified and Cy3-labelled miR-451a probes were designed and synthesised by Genepharma (China); the probe sequence was AAC+TCAGTAA+T-GGTAACGGT+TT; the '+' sign was the modification site of the locked nucleotide. The probe signals were detected with a fluorescence in situ hybridisation (FISH) kit (RiboBio, China) according to the manufacturer's instructions. Briefly, 15 μm thick brain sections were incubated with miR-451a probes for 10 hours at 37°C after treatment with prehybridisation solution. After washing with PBS, some FISH sections were performed following the immunofluorescent procedure as described above.

The primary antibodies included rabbit antineuronal nuclear antigen (NeuN) (1:500; Abcam, ab177487), mouse anti-glial fibrillar acidic protein (GFAP) (1:800; Millipore, MAB360) and rabbit anti-GFAP (1:400; Abcam, ab7260); the secondary antibodies were Alexa Fluor 488 donkey anti-mouse IgG (1:1000; Invitrogen, A21202) and Alexa Fluor 488 donkey anti-rabbit IgG (1:1000; Invitrogen, A21206).

The fluorescent images at 400× magnification were captured by a Zeiss LSM710 confocal microscope (Zeiss, Germany) with a constant exposure time, offset and gain for each fluorescent staining marker from the mPFC. The total fluorescence intensity of CRFR1 or Cy3-labelled miR-451a in the mPFC was quantified by ImageJ V.1.52a (National Institutes of Health) and shown as a ratio normalised to control. Three to four brain sections in each set were averaged for each mouse, and four to five mice were averaged for each group.

Cell culture and transfections

Human embryonic kidney cells (HEK293T) and mouse brain cells (Neuro-2a, N2A) were cultured in Dulbecco's modified eagle's medium supplemented with 10% fetal bovine serum (Gibco), 100 U/mL penicillin and 100 μg/mL streptomycin (Invitrogen, USA) at 37°C with 5% CO_2.

For miR-451a downregulation, an miR-451a antisense hairpin inhibitor (RiboBio) was used. Mature double-stranded miR-451a was designed as a mimic (RiboBio) to imitate the overexpression of miR-451a. For *ATF2* knockdown, an siRNA duplex against mouse *ATF2* or a scrambled negative control was used (Genepharma). Briefly, cells were seeded in 12-well plates at a density of 2×10^5 cells per well. Twenty-four hours after seeding, mimics (50 nM) or inhibitors (100 nM) of miRNA and negative control or ATF2 siRNA (100 nM) were transfected into cells by Lipofectamine 2000 (Invitrogen, USA) following the manufacturer's instructions. Cell RNA and protein were obtained 48 hours after transfection.

Primary cortical neurons were dissociated from postnatal day-1 C57BL/6J mice and cultured at 5×10^6 cells/mL in Neurobasal-A medium (Invitrogen, Carlsbad, California) supplemented with B27 (Invitrogen, USA) and glutamine (Sigma, USA) on substrates precoated with 0.5 mg/mL of poly-L-lysine (Sigma). On the ninth day, the neurons were transfected with miR-451a mimic (75 nM) or an equal amount of scramble sequence using INTERFER in transfection reagent (Polyplus Transfection, PT-409-10) according to the manufacturer's protocol, and then were treated with 10 μm CORT (Selleck, USA) or vehicle (dimethyl sulfoxide (DMSO) at 1:1000 dilution) 6 hours later and continued to be cultured for an additional 3 days. The primary cortical neurons were labelled with the PKH26 red fluorescent cell lipid membrane marker (Sigma) to make the dendritic arbours visible. Three wells were replicated for each treatment, with five different fields of view taken randomly per well using a digital microscope (Zeiss), and spines on dendritic arbours that were at least 50 μm long were analysed.

Dual-luciferase assays

Normal and mutated 3′ untranslated region (UTR) sequences (Atf2 mmu-miR-451a wild type, 5′-GGAA GAATATTAGAAACACTTTTTTTTAAGTGAGTGAAAG TATG GTAA GACG GTTA GTGC TTTG TGCA CTTC TTAGACTAATCAA-3′; Atf2 mmu-miR-451a mutant, 5′-GGAAGAATATTAGAAACACTTTTTTTTAAGTGAGTG AATCATACCAAATTGCAAAGTGCTTTGTGCACTTCT TAGACTAATCAA-3′) of ATF2 were subcloned into the pmirGLO Dual-Luciferase miRNA target expression vector (Tsingke, Nanjing, China). HEK293T cells were transfected with the transfection-ready luciferase reporter construct and the mimics and inhibitors of miR-451a and negative control (50 nM per well). Forty-eight hours after transfection, the cells were lysed and luciferase reporter activities were assayed using the Dual-Luciferase Reporter Assay System (E1910; Promega) according to the manufacturer's protocol. We normalised firefly luciferase activity to Renilla luciferase activity for each sample.

Statistical analysis

Data represent mean±SEM and were analysed using GraphPad Prism V.8.0 software (GraphPad Software, USA). Statistical differences between the two groups were analysed using two-tailed unpaired Student's t-test or Mann-Whitney U test. Normality was determined through Anderson-Darling test for normality. Differences between multiple groups were assessed by one-way or two-way analysis of variance, followed by Tukey's multiple comparison test. The correlation between miR-451a and behavioural indexes was measured by Pearson's correlation analysis. The correlation between miR-451a, miR-1202 in serum, and question 7 (Q7) and question 23 (Q23) in the HAMD of patients with MDD was measured by non-parametric Spearman correlation. P value at 0.05 was considered a statistically significant level.

RESULTS

Screening of miRNAs associated with anhedonia and behavioural hopelessness in patients with MDD and in CRS mice

A variety of miRNAs, such as miR-34a/b/c-5p, miR-101-3p, miR-124-3p, miR-132-3p, miR-182-5p, miR-221-3p, miR-320a-3p, miR-451a and miR-1202, have been reported to be abnormal in the serum or CSF of patients with depression.[4 5 11 12] We measured these miRNAs in serum samples from 35 patients with MDD and found that miR-34a-5p, miR-34c-5p, miR-132-3p, miR-182-5p, miR-221-3p and miR-320-3p increased, miR-451a and miR-1202 decreased, and miR-34b-5p, miR-101-3p and miR-124-3p were unchanged from age-matched healthy controls (figure 2A). The correlation analysis further revealed that the relative levels of serum miR-451a were negatively correlated to the HAMD-24 score (figure 2B) and the Q7 (work and interest) score (online supplemental table S6) but not to the Q23 (feeling of despair) score (online supplemental table S6) or HAMA score (figure 2D). The

relative levels of serum miR-1202 were also negatively correlated to the HAMD-24 score (figure 2C), but not to the Q7, Q23 or HAMA score (online supplemental table S6 and figure 2E). There was no significant correlation between the HAMD-24 score and the relative levels of serum miR-34a-5p, miR-34c-5p, miR-132-3p, miR-182-5p, miR-221-3p or miR-320-3p (online supplemental figure S1A–G). Therefore, in the current study, we further investigated the pathophysiological role of miR-451a in MDD using a CRS mouse model.

The mice subjected to 4 weeks of CRS showed depressive-like behaviours, as demonstrated by reduced sucrose preference, increased immobility in the FST and increased social avoidance (figure 3A–D). However, no obvious anxiety-like abnormalities were observed during the OFT and EPM tests (online supplemental figure S2A–D), consistent with published literature.[13] The serum levels of miR-451a decreased significantly in the CRS mouse model, compared with their intact controls (figure 3E). Moreover, the relative levels of serum miR-451a in CRS mice were negatively correlated to the immobility time in the FST (figure 3F) and positively correlated to the sugar preference rate (figure 3G) and social interaction ratio (figure 3H), respectively, but not with most of the EPM or OFT indexes (online supplemental figure S3A–D). Together, the above results from patients with MDD and the CRS mouse model consistently demonstrated decreases in the serum miR-451a levels and a negative correlation between the relative levels of serum miR-451a and anhedonia.

miR-451a in the mPFC regulated anhedonia and behavioural despair in the CRS mouse model

To explore the neurobiological basis of miR-451a regulating depression, we first observed miR-451a expression in the forebrain of intact mice by RNA FISH. Our results showed that miR-451a signals were mainly distributed in layers 3–5 of the mPFC (online supplemental figure S4A). The high-magnification images revealed that miR-451a was mainly localised to the perikaryon of cortical neurons (online supplemental figure S4B). We then observed the effects of CRS on miR-451a expression in the mPFC of CRS mice. The qPCR results showed that the expression levels of miR-451a decreased in the mPFC of CRS mice (online supplemental figure S5A).

We also screened mice that were susceptible or resistant to CRS through the FST and SPT (online supplemental figure S5B) and demonstrated that the spine loss was more evident in the mPFC of CRS-susceptible mice than in CRS-resistant mice (online supplemental figure S6A,B). Notably, miR-451a levels were lower in the mPFC of CRS-susceptible mice than in CRS-resistant mice (online supplemental figure S5C). FISH results confirmed a significant decrease in miR-451a levels in the mPFC of CRS-susceptible mice compared with intact controls but remained unchanged in CRS-resistant mice (online supplemental figure S5D,E). The expression levels of miR-451a in the hippocampus were not affected
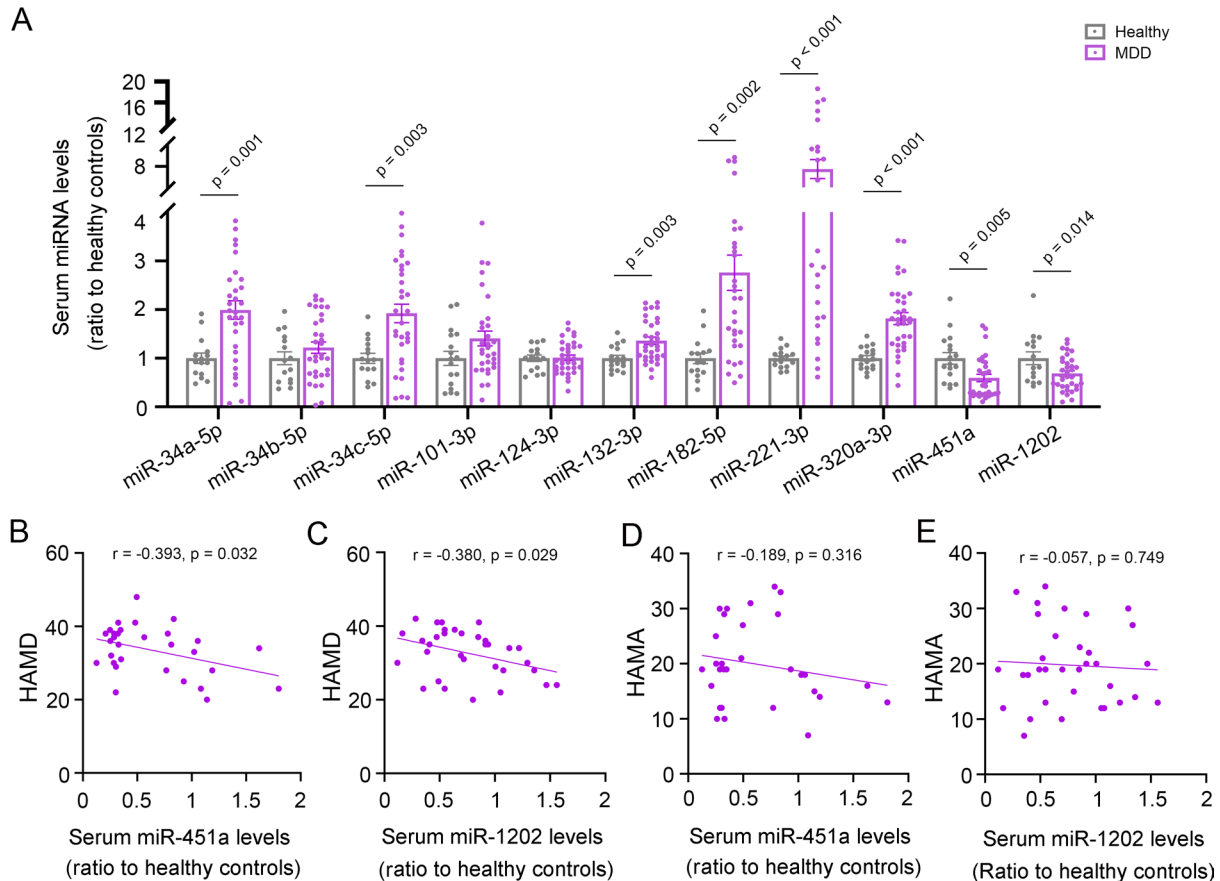
Figure 2 Partially negative correlation between serum miR-451a levels and depressive severity of patients with MDD. (A) The real time-qPCR analysis showed increases in miR-34a-5p, miR-34c-5p, miR-132-3p, miR-182-5p, miR-221-3p and miR-320a-3p levels, no changes in miR-34b-5p, miR-101-3p and miR-124-3p, and decreases in miR-451a and miR-1202 levels in the serum of patients with MDD (n=33), relative to those from the healthy controls (n=15). (B–E) Both relative serum levels of miR-451a and miR-1202 in patients with MDD were partially correlated with the total score of HAMD (B and C) but not with the HAMA score (D and E). Data are mean±SEM and analysed using Student's t-test (A) or Pearson's correlation test (B–E). HAMA, Hamilton Rating Scale for Anxiety; HAMD, Hamilton Rating Scale for Depression; MDD, major depressive disorder; miRNA, microRNA; qPCR, quantitative polymerase chain reaction; SEM, standard error of the mean.

by CRS, with no differences observed between CRS-susceptible mice and CRS-resistant mice (online supplemental figure S7A,B).

We further explored whether exogenous overexpression of miR-451a in the mPFC could ameliorate the CRS-induced, depressive-like phenotype of mice. The AAV9 overexpressing miR-451a was microinjected into the mPFC of 8-week-old mice. After 2 weeks of recovery, these animals underwent CRS for 4 weeks before behavioural tests (figure 4A,B). miR-451a overexpression in the mPFC significantly mitigated the anhedonia and behavioural despair of CRS mice (figure 4C,D). However, the overexpression of miR-451a in the mPFC did not affect social interaction and anxiety-like behaviours in both CRS mice and control mice (online supplemental figure S8A–E). Local injection of AAV9-miR-451a-GFP upregulated the miR-451a gene expression in the mPFC by twofold to threefold, compared with that of the AAV control group, as revealed by real-time qPCR (figure 4E). Immunofluorescence staining demonstrated that AAV9-miR-451a-GFP-infected cells were mainly colocalised with NeuN

(figure 4F,G). The neuropathological analysis demonstrated that the overexpression of miR-451a in the mPFC neurons partially rescued CRS-induced dendritic spine loss (figure 4H,I). Together, these results indicated that miR-451a in the mPFC might serve as a key molecule for the CRS-induced, depressive-like phenotype in mice.

Overexpression of miR-451a in the mPFC normalised elevated CRFR1 expression induced by CRS

Previous studies have shown that impairments of dendritic plasticity in chronic stress-induced depression are associated with disturbances of the hypothalamic-pituitary-adrenal (HPA) axis.[14 15] We also found that CRS-susceptible mice had elevated serum CORT levels (online supplemental figure S6C), increased CRFR1 expression and decreased glucocorticoid receptor (GR) expression in the mPFC, compared with either intact controls or CRS-resistant mice (online supplemental figure S6D). In addition, the corticotropin-releasing factor (CRF) levels were not different between CRS-susceptible and CRS-resistant mice, although they were significantly lower
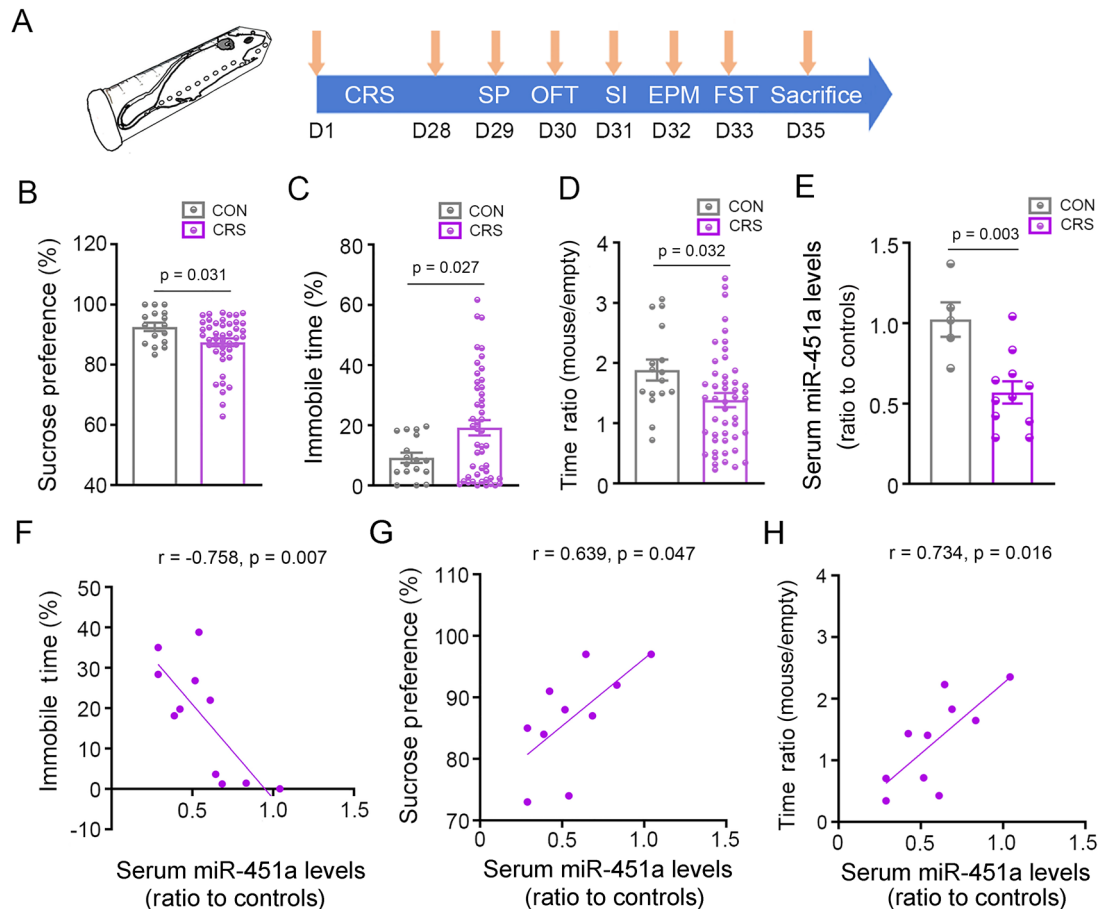
Figure 3 Partially negative correlation between serum miR-451a levels and depressive-like phenotype of CRS mice. (A) The paradigm of CRS and behaviour tests, including SP, OFT, SI, EPM, FST. (B–D) CRS-induced, depression-like behaviours including decreased sugar water preference, increased immobile time of FST and decrease in the ratio of time spent with the congenic mouse in the empty compartment (controls: n=16, CRS: n=46). (E) The quantitative RT-PCR revealed that the serum miR-451a levels were significantly decreased in CRS stress mice (controls: n=5 mice, CRS: n=11 mice). (F–H) The correlation analysis revealed that the serum miR-451a relative levels (ratio to the average of control group) in CRS mice (n=11) were negatively correlated with forced swim immobile time (F), but positively correlated with sugar water preference (G) and the ratio of time spent with the congenic mouse to in the empty compartment (H). Data are mean±SEM and analysed using Student's t-test (B–E) or Pearson's correlation test (F–H). CON, controls; CRS, chronic restraint stress; EPM, elevated plus maze; FST, forced swimming test; miR-451a, microRNA-451a; OFT, open field test; RT-PCR, real-time polymerase chain reaction; SEM, standard error of the mean; SI, social interaction; SP, sucrose preference.

than those of the intact controls (online supplemental figure S6D). Overexpression of miR-451a completely rescued the alterations of CRFR1 and CRF protein levels in the mPFC of CRS mice but had no significant effect on GR levels (online supplemental figure S9A,B). Overexpressing miR-451a in the mPFC also reduced the serum CORT levels of CRS mice (online supplemental figure S9C). Consistently, immunofluorescence staining revealed a significant increase in CRFR1 expression in the mPFC of CRS mice, which was normalised by overexpression of miR-451a (online supplemental figure S9D,E).

In vitro data also demonstrated that CORT-induced spine loss of primary mouse neurons in culture was rescued by miR-451a mimic (online supplemental figure S10A,B). The transcriptional activity and protein level of CRFR1 were significantly inhibited in 293T cells when treated with miR-451a mimic (figure 5A,B). Together, the above data suggested that miR-451a resisted the CRS-induced

dendritic spine loss by maintaining CRFR1 expression in the mPFC.

The inhibitory effect of miR-451a on transcriptional regulation of *CRFR1* via the ATF2/Rela pathway

We further explored the potential mechanisms by which miR-451a inhibits CRFR1 expression. *CRFR1* was not a direct downstream target of miR-451a, as analysed by the TargetScan and miRanda databases, indicating the existence of indirect regulatory mechanisms. Therefore, we determined whether miR-451a regulates the expression of *CRFR1* via its upstream transcription factors. We performed bioinformatics analysis to screen the potential transcription factors that regulate CRFR1 expression. Nuclear factor kappa B subunit 1 (NFκB1) and RELA proto-oncogene, NF-kB subunit (Rela), were predicted to bind to the promoter of CRFR1 and activate its transcription, according to the TRRUST database and published
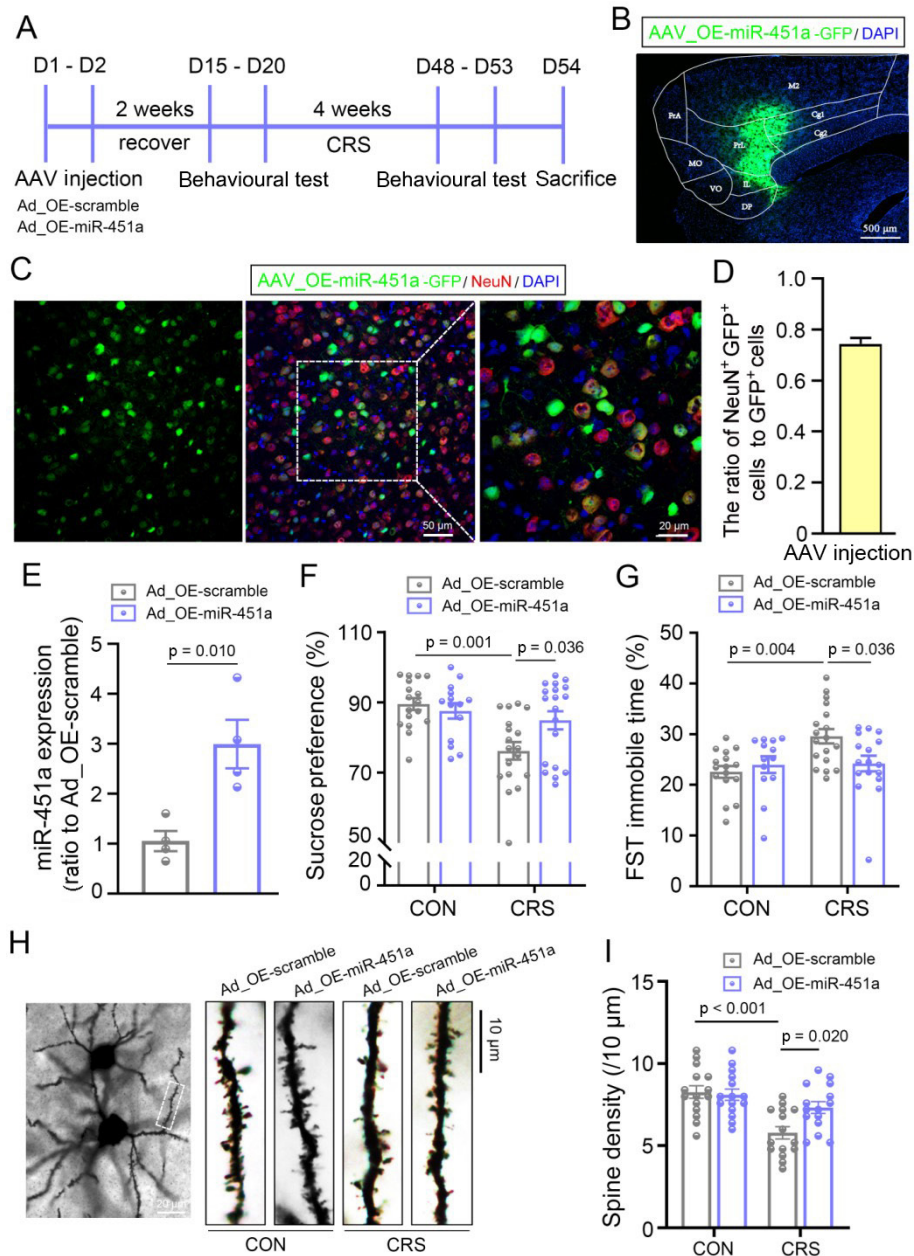
Figure 4 Transgenic overexpression of miR-451a in the mPFC alleviated CRS-induced, depression-like behaviour and neuronal spinal loss in mice. (A) Diagram illustrating the experimental time course for AAV injection (Ad_OE-miR-451a for miR-451a overexpression and Ad_OE-scramble for negative control), CRS model establishment, the behavioural tests and the sacrifice of mice. (B) The representative image of the injected AAV in the mPFC: Cg1, cingulate cortex area 1; Cg2, cingulate cortex area 2; DP, dorsal peduncular cortex; FrA, frontal association cortex; IL, infralimbic cortex; M2, secondary motor cortex; MO, medial orbital cortex; PrL, prelimbic cortex; VO, ventral orbital cortex. (C) Typical fluorescent images of AAV_OE-miR-451a-GFP-infected cells (green) and neurons (red) in the mPFC. (D) The statistical graph shows the percentage of AAV_OE-miR-451a-GFP-infected neurons in total neurons (n=3 mice, 3 slices per mouse). (E) AAV _OE-miR-451a-GFP injection increased miR-451a level in the mPFC (n=4). (F) CRS-induced decrease in sucrose intake preference, which was reversed by prior injection of AAV virus expressing miR-451a (Ad_OE-miR-451a) into the mPFC (Ad_OE-scramble-CON n=17, Ad_OE-miR-451a-CON n=16, Ad_OE-scramble-CRS n=18, Ad_OE-miR-451a-CON n=16). (G) Similarly, overexpression of miR-451a in CRS mice normalised the immobile time in the forced swimming test (Ad_OE-scramble-CON n=17, Ad_OE-miR-451a-CON n=16, Ad_OE-scramble-CRS n=18, Ad_OE-miR-451a-CON n=16). (H) Representative images of dendritic segments and spines of neurons in the mPFC from controls and CRS-exposed mice injected with scrambled and miR-451a overexpression viruses. (I) Quantification revealed that miR-451a overexpression reversed decreases in spine densities of the mPFC neurons of the CRS mice (n=3 per group, 5 neurons per mouse). Data are mean±SEM and analysed by Student's t-test (E) and two-way ANOVA with Tukey post-hoc test (F, G and I), respectively. AAV, adeno-associated virus serotype 9; ANOVA, analysis of variance; CON, control; CRS, chronic restraint stress; DAPI, diamidino-2-phenylindole; FST, forced swimming test; miR-451a, microRNA-451a; mPFC, medial prefrontal cortex; SEM, standard error of the mean.
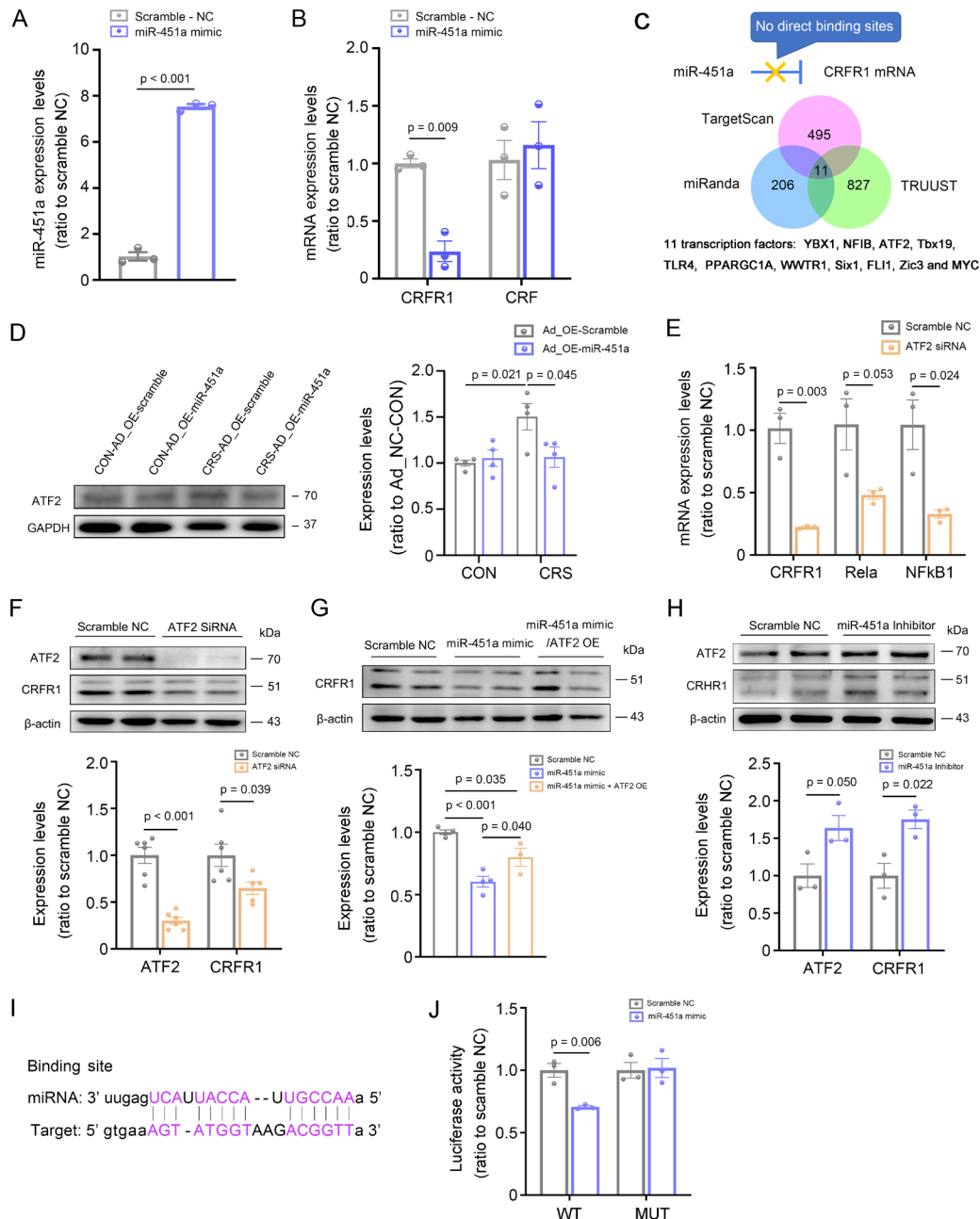
Figure 5 miR-451a negatively regulated CRFR1 transcription by targeting ATF2. (A–B) The quantitative real time-PCR showed that miR-451 expression was dramatically upregulated in 293T cells following the treatment of miR-451a mimic (50 nM) (A), which subsequently decreased the CRFR1 mRNA levels (B) (n=3 per group, each sample in triplicate). (C) Direct targets of miR-451a predicated on TargetScan and miRanda, including 11 transcription factors, but not CRFR1, according to TRRUST database. (D) Western blot showing that overexpression of miR-451a normalised the upregulation of ATF2 protein levels in the mPFC of CRS mice (n=4 per group). (E) The quantitative real time-PCR showed that ATF2 siRNA (100 nM) reduced the mRNA levels of CRFR1, Rela and NFκB1 in N2A cells (n=3 per group, each sample in triplicate). (F) Western blot showing that ATF2 siRNA (100 nM) reduced the protein levels of ATF2 and CRFR1 in N2A cells (n=5–6 per group). (G) Western blot results showing ATF2 overexpression rescued the decreased protein levels of CRFR1 caused by miR-451a mimic (n=3–4 per group). (H) Western blot analysis showing that miR-451a inhibitor (100 nM) increased the protein levels of ATF2 and CRFR1 in N2A cells (n=3 per group). (I) Illustration of nucleotide base pairing between miR-451a and the 3′ UTR of ATF2. (J) Luciferase reporter assay results demonstrated that miR-451a repressed the expression of ATF2 3′ UTR reporter by their seed match. Mutation of the seed match sequence of ATF2 3′ UTR abolished the inhibitory effect of miR-451a (n=3 per group). Data are mean±SEM and analysed using Student's t-test (A, B, E, F and H), one-way ANOVA with Tukey post-hoc test (G) or two-way ANOVA with Tukey post-hoc test (D and J). ANOVA, analysis of variance; ATF2, activating transcription factor 2; CON, control; CRF, corticotropin-releasing factor; CRFR1, corticotropin-releasing factor receptor 1; CRS, chronic restraint stress; GAPDH, glyceraldehyde-3-phosphate dehydrogenase; miR-451a, microRNA-451a; mPFC, medial prefrontal cortex; mRNA, messenger RNA; MUT, mutated; NC, negative control; NFκB1, nuclear factor kappa B subunit 1; PCR, polymerase chain reaction; SEM, standard error of the mean; siRNA, small interfering RNA; UTR, untranslated region; WT, wild type.

reports.[16][17] In addition, 11 transcription factors, including transcription factor 2 (ATF2), were screened out as potential downstream targets of miR-451a (figure 5C). Among them, only ATF2 could transcriptionally activate Rela according to the TRRUST database. Consistently, there was a significant increase in ATF2 expression in the mPFC of CRS mice, which was normalised by overexpression of miR-451a (figure 5D).

To further explore whether *CRFR1* expression was regulated by miR-451a via ATF2, the translation of ATF2 in the N2A cells was blocked by ATF2 siRNA. As expected, the mRNA and protein levels of CRFR1 in N2A cells decreased significantly after the siRNA treatment (figure 5E,F). Meanwhile, the mRNA levels of Rela and NFκB1 also dropped significantly (figure 5E). Moreover, in N2A cells, when treated with an ATF2 overexpression plasmid, the inhibitory effect of the miR-451a mimic on the CRFR1 protein level was abolished (figure 5G). The administration of miR-451a inhibitors in N2A cells increased ATF2 and CRFR1 protein levels (figure 5H), indicating that the homeostasis of CRFR1 in this cell line is regulated by miR-451a. The luciferase reporter gene experiment further demonstrated that miR-451a inhibited the translation of ATF2 mRNA to the protein level by binding to the ATF2 3′ UTR region (figure 5I,J). Together, the above results revealed that miR-451a targeted ATF2 and negatively regulated the transcription of CRFR1 via the ATF2/Rela pathway.

DISCUSSION

MDD, a chronic debilitating disease with a high disability rate, seriously affects the quality of life of patients. Due to the complexity and heterogeneity of the disease, the diagnosis relies primarily on the patient's subjective description, lacking a convincing objective diagnosis basis.[1] Growing evidence has proved that epigenetics, especially miRNAs, bridge the gap between environment and genes. Exploring the regulating mechanism of miRNAs in the onset and pathogenesis of MDD might be beneficial for the prevention, diagnosis and treatment of the disease.[3] Currently, several validated miRNAs associated with MDD have been identified, but the results are often inconsistent and diverging.[4]

Main findings

In the present study, we observed that the levels of miR-451a and miR-1202 were significantly decreased in serum samples from patients with MDD compared with healthy controls. These findings are in line with previous studies.[4][5] However, we did not detect any noticeable changes in the serum levels of miR-34b-5p, miR-101-3p and miR-124-3p in patients with MDD. Additionally, miR-134-5p and miR-383-5p were undetectable in the serum samples, possibly due to their low levels. These discrepancies may be attributed to variations in the patients' genetic backgrounds, sample sizes, testing methodologies and other factors. Therefore, it is essential to enhance the repeatability of miRNA expression profiles in different cohorts of patients with MDD.

We observed a decrease in serum levels of miR-451a in patients with MDD, which showed a negative correlation with the patients' interests and work ability. These findings are generally consistent with several previous studies. For instance, Wan *et al*[18] reported lower serum and CSF levels of miR-451a in patients with MDD who were not undergoing antidepressant treatment compared with those of control patients. In addition, it has been reported that patients with MDD, regardless of antidepressant treatment, exhibit lower levels of serum miR-451a compared with their healthy counterparts. The study also found a negative correlation between serum miR-451a levels and patients' HAMD scores.[4] Importantly, better efficacy of antidepressant treatment with paroxetine was observed in patients who had higher levels of miR-451a. Together, these findings support that serum miR-451a not only serves as a candidate biomarker for MDD diagnosis but also a predictor of response to antidepressant treatment.

Animal studies also demonstrated that miR-451a was downregulated in the rats induced by early-life stress through maternal separation. This downregulation was reversed by both the N-methyl-D-aspartate receptor antagonist ketamine and electroconvulsive shock therapy, indicating a convergent effect.[19] In the CRS-induced mouse model of depression, we observed a significant correlation between the serum level of miR-451a and the levels of despair and euphoria perception in mice. Moreover, the levels of miR-451a in the mPFC differed between susceptible and resistant mice in response to CRS-stimulated depression. Notably, continuously treating the mice with miR-451a via a prior virus injection into the mPFC resulted in resistance to CRS-induced anhedonia and behavioural despair. This antidepressive effect was associated with an improvement in dendritic spine density in the mPFC of CRS mice. Therefore, the above behavioural and pathological evidence further highlights the potential of miR-451a as a target for the treatment of depression.

The overactivation of the HPA axis is involved in the development of MDD. Elevated CORT levels have been shown to cause CRF-CRFR1 disturbance in the central nervous system, subsequently impairing the dendritic and synaptic plasticity.[20] Exposure to corticotropin-releasing hormone (CRH) provoked spine loss and dendritic regression in hippocampal organotypic cultures; rapid spine loss within hours of the onset of stress could be abolished by blocking CRFR1.[21] Consistently, in our study, we observed a significant increase in serum CORT levels following CRS, especially in CRS-susceptible mice. We also observed decreased levels of CRF and increased levels of its receptor CRFR1 in the mPFC of mice after CRS. These findings support a mechanistic role for CRH-CRFR1 signalling in stress-evoked spine loss and dendritic remodelling of mPFC.

Neurons in the mPFC that express CRFR1 have been shown to mediate executive dysfunction induced by acute stress.[22] Chen *et al*[23] characterised CRF-positive neurons

as a unique subtype of GABAergic inhibitory interneurons in mPFC that were directly involved in behavioural despair. Blocking of dorsal mPFC CRF neurons increased anhedonia/behavioural despair and induced social avoidance behaviour, whereas activation had the opposite effect. These results uncover a critical role of mPFC CRF interneurons in bidirectionally controlling motivated behavioural style selection under stress. In our study, we observed upregulation of CRFR1 in mPFC neurons and loss of dendritic spines in CRS-susceptible mice but not in CRS-resistant mice. These findings emphasise the crucial role of CRF/CRFR1 signalling in the mPFC in modulating susceptibility to various chronic stresses.

We further proved that miR-451a could regulate the transcriptional activity of CRFR1 by targeting ATF2/Rela. ATF2, a transcription factor, belongs to the ATF/cAMP-response element binding protein family, characterised by a basic zipper domain consisting of basic amino acids and a leucine zipper that serves as a DNA-binding region. Early studies have reported that long-term stress leads to increased phosphorylation of ATF2 in the brain, especially in the frontal cortex, which could be reduced by antidepressants.[24] In a mouse model of chronic, unpredictable mild stress or lipopolysaccharide-induced depression, ATF2 activation in the hippocampus promoted the neuroinflammatory response associated with the onset of depression by upregulating the transcription of cyclooxygenase-2 (COX-2).[25] The present results reveal that miR-451a targets ATF2 and negatively regulates the transcription of CRFR1, which in turn could regulate neuronal structure plasticity and the homeostasis of the HPA axis following stress.

In addition to regulating the ATF2/Rela pathway, miR-451a has been shown to upregulate mammalian target of rapamycin (mTOR) activity by reducing adenosine monophosphate-activated protein kinase (AMPK) phosphorylation.[26] Ketamine, a rapid-acting antidepressant, has been reported to activate the mammalian target of the rapamycin (mTOR) pathway, leading to increased expression of synaptic protein, dendritic spine density and functional recovery of synapse in the prefrontal cortex.[27] In addition, the antidepressant effect of ketamine has been shown to be abolished by inhibiting mTOR with rapamycin in patients with depression.[28] Therefore, it is worth further exploring whether the AMPK-dependent mTOR signalling pathway is also involved in the antidepressant effects of miR-451a.

Limitations

Due to the relatively small sample size of this study, the conclusions should be considered preliminary. Future research involving a larger sample size is required to substantiate these findings. In the current study, only male mice were selected because male mice were more sensitive to stress-induced, depression-like behaviour than female mice.[29] This gender bias may impede the generalisability of our findings to understand depression mechanisms in females. It is also necessary to explore the aforementioned correlations and mechanisms in different mouse models of depression, which will further elucidate the significant role of miR-451a in depression and its potential as a therapeutic target. In addition, CRFR1 western blot results showed a single band in the mouse prefrontal cortex but two bands in N2A cells. A similar discrepancy was also observed in published literature.[30] This inconsistency in band patterns is likely due to different CRFR1 splicing isoforms in various cell types and species.

Implications

In conclusion, our study reveals that miR-451a levels are reduced in the serum of patients with MDD, a finding that is congruent with prior research. Importantly, our study provides novel insights indicating that the concentration of miR-451a in the mPFC is inversely associated with susceptibility to CRS in mice, particularly in terms of anhedonia and behavioural despair. Mechanistically, miR-451a overexpression could avert dendritic spine loss by modulating the ATF2/Rela pathway in cortical neurons, thereby proposing its potential role as a biomarker and therapeutic target for MDD (online supplemental figure S11).

ORCID iD
Ming Xiao http://orcid.org/0000-0001-5528-9102

REFERENCES

1. Otte C, Gold SM, Penninx BW, *et al*. Major depressive disorder. *Nat Rev Dis Primers* 2016;2:16065.
2. Kendler KS. The genealogy of major depression: symptoms and signs of melancholia from 1880 to 1900. *Mol Psychiatry* 2017;22:1539–53.
3. Willner P. Reliability of the chronic mild stress model of depression: a user survey. *Neurobiol Stress* 2017;6:68–77.
4. Żurawek D, Turecki G. The miRNome of depression. *Int J Mol Sci* 2021;22:11312.
5. Kuang W-H, Dong Z-Q, Tian L-T, *et al*. microRNA-34A-5P, and microRNA-221-3p as predictors of response to antidepressant treatment. *Braz J Med Biol Res* 2018;51:e7212.
6. Camkurt MA, Acar Ş, Coşkun S, *et al*. Comparison of plasma microrna levels in drug naive, first episode depressed patients and healthy controls. *J Psychiatr Res* 2015;69:67–71.
7. Beals J, Novins DK, Spicer P, *et al*. Challenges in operationalizing the DSM-IV clinical significance criterion. *Arch Gen Psychiatry* 2004;61:1197–207.
8. HAMILTON M. A rating scale for depression. *J Neurol Neurosurg Psychiatry* 1960;23:56–62.
9. Zigmond AS, Snaith RP. The hospital anxiety and depression scale. *Acta Psychiatr Scand* 1983;67:361–70.
10. Zhou H-Y, He J-G, Hu Z-L, *et al*. A-kinase anchoring protein 150 and protein kinase a complex in the basolateral amygdala contributes to depressive-like behaviors induced by chronic restraint stress. *Biol Psychiatry* 2019;86:131–42.
11. Fang Y, Qiu Q, Zhang S, *et al*. Changes in miRNA-132 and miR-124 levels in non-treated and citalopram-treated patients with depression. *J Affect Disord* 2018;227:745–51.
12. Lopez JP, Lim R, Cruceanu C, *et al*. Is a primate-specific and brain-enriched microRNA involved in major depression and antidepressant treatment. *Nat Med* 2014;20:764–8.
13. Pignatelli M, Tejeda HA, Barker DJ, *et al*. Cooperative synaptic and intrinsic plasticity in a disynaptic limbic circuit drive stress-induced anhedonia and passive coping in mice. *Mol Psychiatry* 2021;26:1860–79.
14. Gold SM, Krüger S, Ziegler KJ, *et al*. Endocrine and immune substrates of depressive symptoms and fatigue in multiple sclerosis patients with comorbid major depression. *J Neurol Neurosurg Psychiatry* 2011;82:814–8.
15. Lamers F, Vogelzangs N, Merikangas KR, *et al*. Evidence for a differential role of HPA-axis function, inflammation and metabolic syndrome in melancholic versus atypical depression. *Mol Psychiatry* 2013;18:692–9.
16. Zocco D, McMorrow JP, Murphy EP. Histamine modulation of peripheral CRH receptor type 1alpha expression is dependent on Ca(2+) signalling and NF-kappaB/P65 transcriptional activity. *Mol Immunol* 2010;47:1426–37.
17. Cuhlmann S, Van der Heiden K, Saliba D, *et al*. Disturbed blood flow induces rela expression via C-Jun N-terminal kinase 1 a novel mode of NF-Kappa B regulation that promotes arterial inflammation. *Circ Res* 2011;108:950–9.
18. Wan Y, Liu Y, Wang X, *et al*. Identification of differential microRNAs in cerebrospinal fluid and serum of patients with major depressive disorder. *PLoS One* 2015;10:e0121975.
19. O'Connor RM, Grenham S, Dinan TG, *et al*. microRNAs as novel antidepressant targets: converging effects of ketamine and electroconvulsive shock therapy in the rat hippocampus. *Int J Neuropsychopharmacol* 2013;16:1885–92.
20. Wang X-D, Chen Y, Wolf M, *et al*. Forebrain Crhr1 deficiency attenuates chronic stress-induced cognitive deficits and dendritic remodeling. *Neurobiol Dis* 2011;42:300–10.
21. Chen Y, Dubé CM, Rice CJ, *et al*. Rapid loss of dendritic spines after stress involves derangement of spine dynamics by corticotropin-releasing hormone. *J Neurosci* 2008;28:2903–11.
22. Uribe-Mariño A, Gassen NC, Wiesbeck MF, *et al*. Prefrontal cortex corticotropin-releasing factor receptor 1 conveys acute stress-induced executive dysfunction. *Biol Psychiatry* 2016;80:743–53.
23. Chen P, Lou S, Huang Z-H, *et al*. Prefrontal cortex corticotropin-releasing factor neurons control behavioral style selection under challenging situations. *Neuron* 2020;106:301–15.
24. Laifenfeld D, Karry R, Grauer E, *et al*. Atf2, a member of the CREB/ATF family of transcription factors, in chronic stress and consequent to antidepressant treatment: animal models and human post-mortem brains. *Neuropsychopharmacology* 2004;29:589–97.
25. Song Q, Fan C, Wang P, *et al*. Hippocampal CA1 βCaMKII mediates neuroinflammatory responses via COX-2/PGE2 signaling pathways in depression. *J Neuroinflammation* 2018;15:338.
26. Chen M-B, Wei M-X, Han J-Y, *et al*. Microrna-451 regulates AMPK/Mtorc1 signaling and Fascin1 expression in HT-29 colorectal cancer. *Cell Signal* 2014;26:102–9.
27. Li N, Lee B, Liu R-J, *et al*. mTOR-dependent synapse formation underlies the rapid antidepressant effects of NMDA antagonists. *Science* 2010;329:959–64.
28. Yu J-J, Zhang Y, Wang Y, *et al*. Inhibition of calcineurin in the prefrontal cortex induced depressive-like behavior through mTOR signaling pathway. *Psychopharmacology* 2013;225:361–72.
29. Yang F, Tao J, Xu L, *et al*. Estradiol decreases rat depressive behavior by estrogen receptor beta but not alpha: no correlation with plasma corticosterone. *Neuroreport* 2014;25:100–4.
30. Zegers-Delgado J, Aguilera-Soza A, Calderón F, *et al*. Type 1 corticotropin-releasing factor receptor differentially modulates neurotransmitter levels in the nucleus accumbens of juvenile versus adult rats. *Int J Mol Sci* 2022;23:10800.

Panpan Hu obtained her bachelor's degree of medicine from Guangzhou University of Chinese Medicine, China in 2014. From 2015 to 2021, she conducted scientific research and training in the Key Laboratory of Neurodegenerative Diseases of Jiangsu Province and obtained her doctorate degree in pharmacology from Nanjing Medical University in China. She has been working in the Department of Anesthesia Pharmacology at the Naval Medical University in China since 2021. Her main research interests include the pathogenesis and early diagnosis of depression and neuroprotection of anesthetic drugs.